

RESEARCH ARTICLE

Three-dimensional radiological anatomy of condyle trabecular bone based on a Volume-of-Interest analysis

^{1,2}Fan Li, ¹Xiangliang Xu, ³Qiguo Rong, ⁴Jianwei Wang, ³Jiwu Zhang, ⁵Wen Zhou, ⁴Weiguang Zhang and ¹Chuanbin Guo

¹Department of Oral and Maxillofacial Surgery, National Center of Stomatology & National Clinical Research Center for Oral Diseases & National Engineering Research Center of Oral Biomaterials and Digital Medical Devices, Peking University School and Hospital of Stomatology, Beijing, China; ²Department of Stomatology, Beijing Haidian Hospital, Beijing, China; ³Department of Mechanics and Engineering Science, College of Engineering, Peking University, Beijing, China; ⁴Department of Human Anatomy & Histology and Embryology, Peking University Health Science Center, Beijing, China; ⁵Department of Central Laboratory, National Center of Stomatology & National Clinical Research Center for Oral Diseases & National Engineering Research Center of Oral Biomaterials and Digital Medical Devices, Peking University School and Hospital of Stomatology, Beijing, China

Objectives: Three-dimensional radiological anatomic characteristics of condyle trabeculae was obtained quantitatively based on a volume-of-interest (VOI) analysis.

Methods: Nine human mandibular condyle specimens were scanned by micro-computed tomography (micro-CT). A total of 34 VOIs were selected from each condyle specimen, which were divided into six layers and four parts to analyze the morphological characteristics of trabeculae based on cylindrical VOIs with a diameter and height of 2mm. One-way analysis of variance was used to compare the regional differences of morphological parameters among each layer and part.

Results: Values for bone mineral density, bone volume/total volume, trabecular thickness, and trabecular bone number were greater in the anterior part compared with the posterior part; and the lateral part was larger than the medial part in the first, second, and third layers, while the medial part was larger in the fourth and fifth layers; these values in the first and sixth layers were much larger, while those in the third and fourth layers were smaller. Bone surface area/bone volume, trabecular spacing, and trabecular bone pattern factor were larger in the posterior part than in the anterior part; and the lateral part was larger than the medial part in the fourth and fifth layers, while the medial part was larger in the first and second layers.

Conclusions: The morphological distribution of VOIs was anisotropic within trabecular bone of human mandibular condyles. The upper and lower ends of trabecular bone were much more compact, with higher bone density, trabecular thickness, and trabecular number than in the middle layers.

Dentomaxillofacial Radiology (2022) **51**, 20220138. doi: [10.1259/dmfr.20220138](https://doi.org/10.1259/dmfr.20220138)

Cite this article as: Li F, Xu X, Rong Q, Wang J, Zhang J, Zhou W, et al. Three-dimensional radiological anatomy of condyle trabecular bone based on a Volume-of-Interest analysis. *Dentomaxillofac Radiol* (2022) 10.1259/dmfr.20220138.

Keywords: mandibular condyle; trabecular bone; Micro-CT; anatomy

Introduction

The temporomandibular joint (TMJ) is the only combined bilateral joint. The TMJ plays a crucial role in activities such as swallowing, mastication, and speech.^{1,2}

The configuration of the condyle is irregular, and the condyle microstructure is comprised of thin cortical bone and spongy trabecular bone, which is mainly rod- and plate-like.³ Load is transmitted from cortical bone to trabecular bone during functional movement of the mandible. Wolff's law indicated that bone structure was changed by mechanical stimulation during bone

Correspondence to: Chuanbin Guo, E-mail: guodazuo@vip.sina.com; Weiguang Zhang, E-mail: zhangwg@bjmu.edu.cn

Received 17 April 2022; revised 13 June 2022; accepted 17 June 2022

The authors Fan Li and Xiangliang Xu contributed equally to the work.

growth, which implied that trabecular bone tended to be arranged along the main pressure direction. There could be an adaptive relationship between the morphological structure and mechanical properties of bone in different positions.⁴

Micro-computed tomography (micro-CT) was developed in the 1990s and can be used to develop images with relatively a higher spatial resolution than that obtained with conventional CT, and it is relatively low-cost and convenient.⁵ Micro-CT can be used to obtain detailed three-dimensional information about the spatial structure and organization of bone as well.⁶ With image processing software, researchers could observe the details of tomographic images and obtain three-dimensional surface images, which made it possible to evaluate the morphology and mechanical properties of trabecular bone.⁷ Ebrahim *et al* reported that cone-beam CT could help to characterize the internal structure of mandibular condyle trabecular bone; while, micro-CT afforded a relatively higher resolution and accuracy than those afforded by cone-beam CT.⁸

Previous research into the microstructure of human condyle trabecular bone only characterized the two-dimensional distribution, specific three-dimensional anatomical features had not been disclosed. This study aimed to investigate the anatomical morphology and radiological information of the TMJ by conducting a three-dimensional analysis of human mandibular condyle trabecular bone by using micro-CT. The findings of this study would aid in the research on TMJ diseases and treatments, such as the designment of mandibular condyle prostheses.

Materials & methods

Condyle specimens

Nine human mandibular condyles of cadavers were analyzed (mean age, 68 ± 15 years; age range, 69–85 years), which were donated by the Department of Human Anatomy & Histology and Embryology, Peking University Health Science Center, and informed consent was obtained. The body donation numbers of the nine specimens were BMU990106(#1), BMU990376(#2), BMU990713(#3), BMU990850(#4), BMU2011113(#5), BMU2013040(#6), BMU2014028(#7), BMU2015105(#8), and BMU2015121(#9). The work had been approved by the appropriate ethical committee related to the Peking University Health Science Center,

where this study was performed (IRB00001052-21011-E). The mandibular condyles had a normal morphology without obvious erosion and resorption of the condyle surface. A horizontal cut was made through the lowest point of the sigmoid notch, parallel to the lower border of the mandible, and the specimens were fixed with formalin. The height of the specimens was the vertical distance between the bottom and top of the condyle parallel to the section. The size of the specimens is shown in [Table 1](#).

Micro-computed tomography

In this study, micro-CT (Inveon MM CT, SIEMENS, Munich, Germany) was used to visualize the three-dimensional structure of mandibular condyle trabecular bone. The micro-CT examination of each bone specimen was performed using an Inveon® Multi-Modality gantry (Inveon™ Acquisition Workplace, 1.5.0.28, SIEMENS, Munich, Germany). Specimens were placed on the holder between the X-ray source and the charge-coupled device camera so that the whole specimen was encompassed in the field of view. The scanning parameters were 80 kV, 500 μ A, and a 1500 ms integration time with a selected nominal isotropic resolution of 13.76 μ m. Projection data were then reconstructed with Inveon Research Workplace to create three-dimensional images. The threshold range of this study was 1840–2230, and the mean value was 2019, which separated trabecular bone from marrow spaces.

Volume of interest

Cylindrical volumes of interest (VOIs) were selected from the three-dimensional images of condyle trabecular bone with a diameter and height of 2 mm ([Figure 1](#)), which were perpendicular to the maximum mediolateral and anteroposterior diameter of the condyle. The research scope was that the number of optional VOIs was >3 from top to bottom, which was divided into six equal layers, and then, VOIs of 2 mm in thickness were selected from the center of each part. Within the trabecular bone of the condyles, the maximum number of VOIs that could be jointly selected in all specimens was distributed into six layers from top to bottom, with a total of 34 VOIs, and the VOIs were independent of each other. Each of the layers was separated into four parts: anterior, posterior, medial, and lateral ([Figure 2](#)). When two VOIs could be selected out in the anteroposterior direction, they would be separated into anterior

Table 1 The mediolateral diameter, anteroposterior diameter, and height of the nine specimens

	#1	#2	#3	#4	#5	#6	#7	#8	#9
Mediolateral Diameter(mm)	18.85	20.97	18.60	21.78	20.98	17.10	19.79	20.23	20.26
Anteroposterior Diameter(mm)	11.75	7.41	9.67	11.06	9.41	7.51	10.77	9.48	12.15
Height(mm)	17.73	22.40	22.34	16.87	17.19	19.20	17.00	18.41	18.39

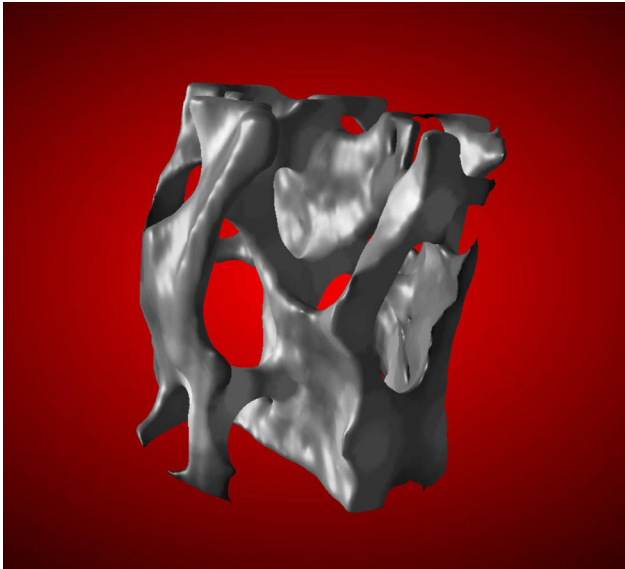


Figure 1 Cylindrical VOIs with a diameter and height of 2mm.

and posterior parts. When only one VOI was selected out in the anteroposterior direction, the VOI close to the medial side-of the condyle was divided into the medial part, and the one close to the lateral side-was divided into the lateral part. In each specimen, 34 VOIs were selected with six layers from the top to the bottom of the condyle. The number of VOIs in each layer was as follows: four VOIs in the first, fourth, fifth, and sixth layers; ten VOIs in the second layer; and eight VOIs in the third layer. VOIs were three-dimensionally

distributed and consistent with the anatomical contour of the condyle. The mean value of each morphological parameter of the VOIs in the nine samples was depicted using color. The black, white, and red circles represent the maximum, minimum, and central transition values of each morphological parameter, respectively. The scope of the color was equally divided into 255 parts to correspond to the value, so the value of the morphological parameter of each VOI could be expressed as color in the scope.

Bone structure

The morphology parameters of the VOIs were analyzed using the software package of the micro-CT system (Inveon™ Acquisition Workplace, 1.5.0.28). Morphology was described by examining bone mineral density (BMD), bone volume/total volume (BV/TV), trabecular thickness (Tb.Th), trabecular bone number (Tb.N), trabecular spacing (Tb.Sp), bone surface area/bone volume (BS/BV), and trabecular bone pattern factor (Tb.Pf). BMD was referred to the mass of mineral per volume of bone, which an important indicator of bone strength and bone mass. By the measurement of BMD, the changes of bone mass could be observed, which was conducive to the early diagnosis, treatment, and prognosis of bone-related diseases.⁹ Comparing the gray values in the trabecular bone with gray values of a CT phantom of known densities attached to micro-CT, the mean BMD of the VOI in the trabecular bone could be calculated. Color scope was used to display the values for each parameter as mentioned above.

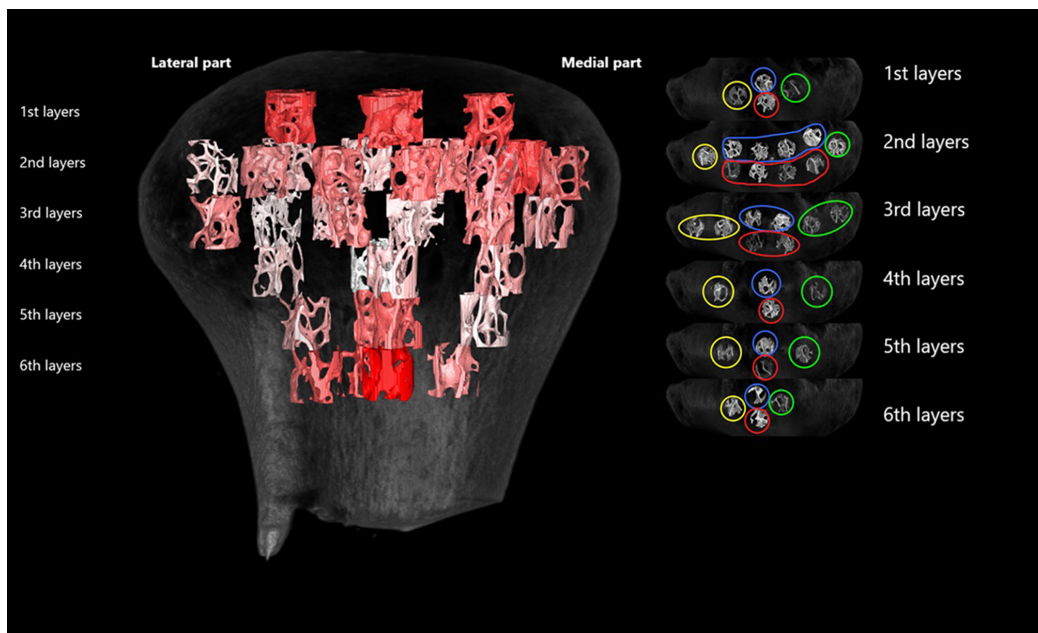


Figure 2 The panel on the left showed the 3D distribution of VOIs. The panel on the right showed the partition of VOIs in transverse views. The yellow circles represented the lateral parts, the green circles represented the medial parts, the blue circles represented the anterior parts, and the red circles represented the posterior parts.

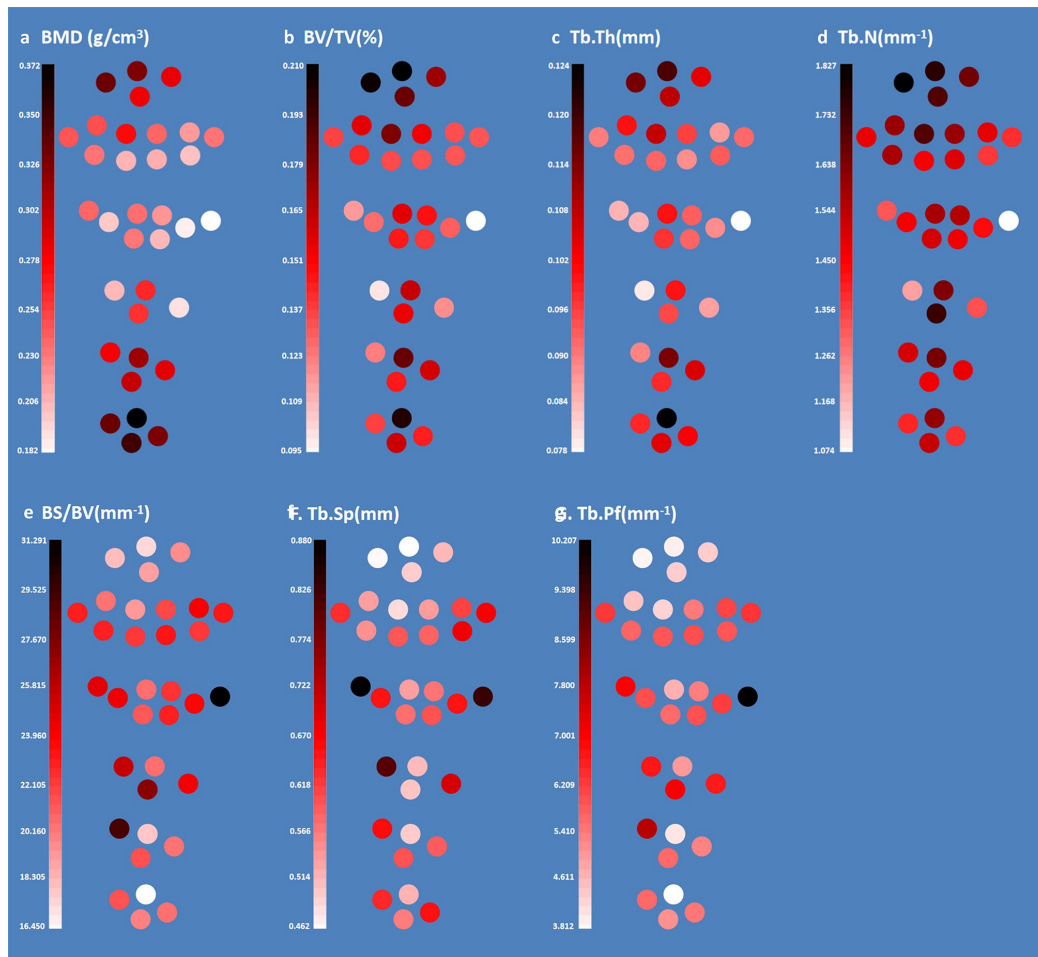


Figure 3 The color scope of the mean value of each VOI for each morphological parameter. The partitions and layers of VOIs were corresponding to the right panel in Figure 2. A. BMD; B. BV/TV; C. Tb.Th; D. Tb.N; E. BS/BV; F. Tb.Sp; G. Tb.Pf.

Statistical analysis

One-way analysis of variance was used to compare the regional differences of each morphological parameter in each VOI between each layer and part. All tests were conducted using IBM SPSS Statistics 26 (IBM Corp., Armonk, NY, USA). The data were in accordance with normal distribution and equal variance. A P value of < 0.05 was considered statistically significant.

Results

The volume of 34 VOIs accounted for 12.26–29.14% of the total volume of trabecular bone. The panels in Figure 3 indicated that the three-dimensional distribution of condyle trabecular bone was anisotropic.

Bone mineral density

BMD in the lateral part of trabecular bone was greater compared with BMD in the medial part in the first, second, third, and sixth layers, while BMD was greater in the medial part compared with the lateral part in the

fourth layer. BMD in the anterior part of trabecular bone was greater compared with BMD in the posterior part in the first, second, and fifth layers, while BMD was greater in the posterior part compared with the anterior part in the fourth layer. BMD in the first, fifth, and sixth layers was much greater compared with BMD in the third and fourth layers.

Bone volume/total volume

BV/TV in the lateral part of trabecular bone was greater when compared with BV/TV in the medial part in the first and third layers, while BV/TV were greater in the medial part compared with the lateral part in the fifth layer. BV/TV in the anterior part were greater compared with BV/TV in the posterior part in each layer. BV/TV in the first and sixth layers were much greater compared with the values in the third and fourth layers.

Trabecular thickness

Tb.Th in the lateral part of trabecular bone was greater compared with Tb.Th in the medial part in the first

and third layers, while Tb.Th was greater in the medial compared with the lateral part in the fourth, fifth, and sixth layers. Tb.Th in the anterior part was greater compared with the posterior part in the first, second, third, fifth, and sixth layers. The values in the first and sixth layers were much greater compared with the values in the third and fourth layers.

Trabecular bone number

Tb.N in the lateral part of trabecular bone was greater compared with the medial part in the third layer, while Tb.N was greater in the medial part compared with the lateral part in the fifth layer. Tb.N in the anterior part of trabecular bone was greater compared with the posterior part in the second, third, and fifth layers. Tb.N in the first and sixth layers was much greater compared with Tb.N in the third and fourth layers.

Trabecular spacing

Tb.Sp in the lateral part was larger than in the medial part in the fourth and fifth layers. Tb.Sp was larger in the posterior part compared with the anterior part in the second, third, fifth, and sixth layers. Tb.Sp in the third and fourth layers was much larger compared with Tb.Sp in the first and sixth layers.

Bone surface arealbone volume

BS/BV was greater in the lateral part compared with the medial part in the fourth, fifth, and sixth layers, while BS/BV was greater in the medial part compared with the lateral part in the first layer. BS/BV was greater in the posterior part compared with the anterior part in the first, second, fifth, and sixth layers. The BS/BV values in the third and fourth layers were much greater compared with the BS/BV values in the first and sixth layers.

Trabecular bone pattern factor

The Tb.Pf in the lateral part was larger compared with the medial part in the second layer, while the Tb.Pf was larger in the medial part than in the lateral part in the first, third, fifth, and sixth layers. The Tb.Pf was larger in the posterior part compared with the anterior part in the first, second, fifth, and sixth layers. The Tb.Pf in the

third and fourth layers was much larger compared with the Tb.Pf in the first and sixth layers.

There were significant differences in all morphological parameters among the six layers (Table 2). Among four parts, Tb.Sp was statistically different in the third layer; BV/TV, Tb.Th, Tb.N, BS/BV and Tb.Sp were statistically different in fourth layer ; Tb.N was statistically different in fifth layer; differences in first, second and sixth layers showed no statistically significant (Table 3).

Discussion

The mandibular condyle is an important component of the TMJ that bear the loads of the mandible during functional movement. Previous studies showed that there was a relationship between the morphological structure and mechanical properties of bone in different positions.⁴ Du et al reported that the correlations between microstructure and mechanical behavior of trabecular bone were consistent at the distal tibia.¹⁰ Therefore, exploring the three-dimensional morphological structure of condylar trabecular bone was conducive to the analysis of its mechanical properties, which would aid in the research on the reconstruction of mandibular condyle defect.

The technique of micro-CT was utilized in most studies of the morphology of human mandibular condyle trabecular bone.¹¹⁻¹⁵ The spatial resolution of micro-CT was relatively high, which could afford clear visualization of the internal microstructure of trabecular bone.⁷ While, the researchers selected less than 9 VOIs in each condyle, which were distributed in one- or two-dimensional directions, to characterize the microstructure of condyle trabecular bone.¹¹⁻¹⁵ Differences between the anterior and posterior parts of trabecular bone were not analyzed in these studies. Although Hongo et al studied the distribution characteristics of the anterior and posterior parts of trabecular bone, they carried out histological techniques to research the trabecular bone.¹⁶ The tissue-based sectioning method only provided a single-layer image with clear trabecular bone structure, and the process was complicated. In this

Table 2 Comparisons of morphological parameters among the six layers

Layers	first layer Mean ± SD)	second layer Mean ± SD)	third layer Mean ± SD)	fourth layer Mean ± SD)	fifth layer Mean ± SD)	sixth layer Mean ± SD)	P
BMD g·cm ⁻³)	0.306 ± 0.489	0.232 ± 0.250	0.214 ± 0.264	0.231 ± 0.355	0.295 ± 0.296	0.345 ± 0.300	0.000*
BV/TV %)	0.194 ± 0.060	0.144 ± 0.046	0.133 ± 0.051	0.136 ± 0.053	0.155 ± 0.061	0.162 ± 0.061	0.000*
Tb.Th mm)	0.111 ± 0.022	0.094 ± 0.019	0.090 ± 0.021	0.090 ± 0.023	0.101 ± 0.028	0.107 ± 0.025	0.000*
Tb.N mm ⁻¹)	1.739 ± 0.347	1.516 ± 0.281	1.427 ± 0.377	1.481 ± 0.390	1.528 ± 0.420	1.480 ± 0.295	0.001*
BS/BV mm ⁻¹)	18.717 ± 3.402	22.245 ± 4.672	23.918 ± 9.238	24.428 ± 11.588	22.343 ± 12.154	19.656 ± 4.393	0.006*
Tb.Sp mm)	0.488 ± 0.132	0.593 ± 0.160	0.665 ± 0.349	0.635 ± 0.231	0.591 ± 0.167	0.597 ± 0.162	0.008*
Tb.Pf mm ⁻¹)	4.211 ± 1.281	5.680 ± 1.897	6.620 ± 4.039	6.388 ± 3.809	5.776 ± 3.851	5.050 ± 1.967	0.006*

(P* < 0.05)

Table 3 Statistics of morphological parameters of trabecular bone at four parts in each layer

Layers	Parts	BMD ($g \cdot cm^{-3}$)	BV/TV (%)	Tb.Th (mm)	Tb.N (mm^{-1})	BS/BV (mm^{-1})	Tb.Sp (mm)	Tb.Pf (mm^{-1})
1	A	0.325 ± 0.025	0.210 ± 0.017	0.117 ± 0.007	1.764 ± 0.098	17.558 ± 1.501	0.462 ± 0.058	4.021 ± 0.607
	L	0.332 ± 0.025	0.207 ± 0.017	0.114 ± 0.007	1.827 ± 0.098	18.364 ± 1.501	0.468 ± 0.058	3.937 ± 0.607
	M	0.286 ± 0.025	0.174 ± 0.017	0.104 ± 0.007	1.660 ± 0.098	19.765 ± 1.501	0.519 ± 0.058	4.434 ± 0.607
	P	0.283 ± 0.025	0.186 ± 0.017	0.107 ± 0.007	1.705 ± 0.098	19.180 ± 1.501	0.503 ± 0.058	4.451 ± 0.607
2	A	0.245 ± 0.012	0.157 ± 0.008	0.097 ± 0.003	1.598 ± 0.049	21.442 ± 0.751	0.547 ± 0.029	5.133 ± 0.304
	L	0.246 ± 0.025	0.137 ± 0.017	0.090 ± 0.007	1.481 ± 0.098	22.949 ± 1.501	0.634 ± 0.058	6.293 ± 0.607
	M	0.234 ± 0.025	0.133 ± 0.017	0.092 ± 0.007	1.381 ± 0.098	23.178 ± 1.501	0.678 ± 0.058	6.353 ± 0.607
	P	0.215 ± 0.012	0.136 ± 0.008	0.091 ± 0.003	1.476 ± 0.049	22.650 ± 0.751	0.606 ± 0.029	5.907 ± 0.304
3	A	0.229 ± 0.018	0.153 ± 0.012	0.096 ± 0.005	1.570 ± 0.069	21.515 ± 1.061	0.558 ± 0.041*	5.105 ± 0.429
	L	0.229 ± 0.018	0.128 ± 0.012	0.087 ± 0.005	1.456 ± 0.071	23.825 ± 1.092	0.638 ± 0.042*	6.079 ± 0.442
	M	0.186 ± 0.018	0.119 ± 0.012	0.087 ± 0.005	1.326 ± 0.071	23.843 ± 1.092	0.751 ± 0.042*	6.646 ± 0.442
	P	0.220 ± 0.018	0.143 ± 0.012	0.095 ± 0.005	1.493 ± 0.069	22.110 ± 1.061	0.592 ± 0.041*	5.839 ± 0.429
4	A	0.263 ± 0.025	0.165 ± 0.017*	0.100 ± 0.007*	1.639 ± 0.098*	20.649 ± 1.501*	0.517 ± 0.058*	5.084 ± 0.607
	L	0.208 ± 0.025	0.100 ± 0.017*	0.080 ± 0.007*	1.213 ± 0.098*	25.612 ± 1.501*	0.808 ± 0.058*	6.716 ± 0.607
	M	0.194 ± 0.025	0.120 ± 0.017*	0.087 ± 0.007*	1.330 ± 0.098*	24.200 ± 1.501*	0.705 ± 0.058*	6.664 ± 0.607
	P	0.273 ± 0.026	0.168 ± 0.018*	0.104 ± 0.007*	1.601 ± 0.104*	19.931 ± 1.592*	0.532 ± 0.061*	4.780 ± 0.644
5	A	0.314 ± 0.025	0.186 ± 0.017	0.113 ± 0.007	1.651 ± 0.098*	18.102 ± 1.501	0.504 ± 0.058	4.149 ± 0.607
	L	0.288 ± 0.026	0.129 ± 0.018	0.098 ± 0.007	1.278 ± 0.104*	21.943 ± 1.592	0.710 ± 0.061	5.666 ± 0.644
	M	0.287 ± 0.025	0.162 ± 0.017	0.105 ± 0.007	1.481 ± 0.098*	20.55 ± 1.501	0.594 ± 0.058	5.378 ± 0.607
	P	0.299 ± 0.025	0.147 ± 0.017	0.098 ± 0.007	1.471 ± 0.098*	21.542 ± 1.501	0.603 ± 0.058	5.684 ± 0.607
6	A	0.372 ± 0.025	0.202 ± 0.017	0.124 ± 0.007	1.606 ± 0.098	16.45 ± 1.501	0.524 ± 0.058	3.812 ± 0.607
	L	0.333 ± 0.025	0.138 ± 0.017	0.098 ± 0.007	1.397 ± 0.098	21.438 ± 1.501	0.638 ± 0.058	5.681 ± 0.607
	M	0.326 ± 0.025	0.145 ± 0.017	0.102 ± 0.007	1.381 ± 0.098	20.606 ± 1.501	0.657 ± 0.058	5.524 ± 0.607
	P	0.349 ± 0.025	0.164 ± 0.017	0.104 ± 0.007	1.534 ± 0.098	20.130 ± 1.501	0.568 ± 0.058	5.185 ± 0.607

A, anterior; L, lateral; M, medial; P, posterior.

*Indicated with bold were found statistically significant ($P < 0.05$).

study, the distribution of three-dimensional radiological morphologic characteristics of trabecular bone of the human mandibular condyle was analyzed more detailed with Micro-CT.

In the literatures related to the micro-CT studies of the condyle trabecular bone, the size of the VOIs varied from 2.48 to 5.00 mm, the number of VOIs was less than 9, and meanwhile, the distribution of the VOIs had not shown the anteroposterior distribution.^{11–15} In this study, a method for analyzing the anatomical characteristics of human condyle trabecular bone was proposed based on 34 cylinder VOIs with a height and diameter of 2 mm, which was divided into 6 layers and four parts as anterior, posterior, medial, and lateral parts. Previous studies showed that the mean anteroposterior diameter of the condyle was 7.72–11.49 mm, and the mean mediolateral diameter was 15.66–21.80 mm.^{17–21} In agreement with these studies, the anteroposterior diameter of the condyle was 7.41–12.15 mm, and the mediolateral diameter was 17.10–21.78 mm in our study.

Compared with the known data from previous studies, the results in this study were consistent with them. The values of BMD, and Tb.Th in this study were much higher at the anterior part than the posterior part, which was corresponding well with the results reported

by Hongo *et al.*¹⁶ The values of BV/TV and Tb.Th in the present study were much higher at the upper and lower ends of trabecular bone than the middle layers, which was corresponding well with the results reported by Giessen *et al.*¹⁵ Besides above, it was also found in this study that the values of BS/TV, Tb.Sp, and Tb.Pf were larger in the posterior part than in the anterior part; and the lateral part was larger than the medial part in the fourth and fifth layers, while the medial part was larger in the first and second layers.

Based on the studies about the microstructure of trabecular bone, it was disclosed that the distribution characteristics of different species and sites were obviously different. The present study for human condyle showed that the value of BV/TV was greater in the lateral part than the medial part in the first and third layers, while smaller in the lateral part than the medial part in the fifth layer, and the value of BV/TV in the first and sixth layers were much greater than the third and fourth layers. This result was not correspond with the distribution characteristic of pig femoral trabecular bone reported by Guo *et al.*, which showed that the value of BV/TV gradually decreased from top to bottom, and was larger in the central area than peripheral area.²² For human distal tibia, Du *et al.* found the values of BV/

TV, Tb.Th, and Tb.N were higher in medial and posterior regions, which was also different from mandibular condyle.¹⁰ These results implied that the differences should be noted when referring to the microstructure parameter of trabecular bone of other species or parts.

Some researchers noted that the morphological parameters that were most suitable to identify subtle changes in the shape of trabeculae could better predict the mechanical properties of bone than those that provide a value for overall connectivity or degree of anisotropy.²³ Goulet and Saers *et al* found strong correlations between the independent structural measures of BV/TV, Tb.Th, and connectivity; BV/TV was also found to be highly correlated with apparent density and ash weight density, high BV/TV, Tb.Th, and low connectivity, and BS/BV was associated with high levels of mechanical strain.^{24,25} At present, three-dimensional printing techniques of porous metal materials had gradually gained acceptance in medicine. Some studies had shown that the porous metal scaffold could reduce the stress-shielding effects between the material and the bone tissue and promote osseointegration.^{26,27} Xu *et al* previously studied artificial condyles with trabecular characteristics, they proposed and investigated a novel tetrahedral structural design of the open porous titanium scaffold to fabricate the trabecula architecture within the condyle, which was also optimized to closely match the Young's modulus of bone, consequently reducing the stress-shielding effect in the finite element model. Their findings showed that the trabecular bone in the lateral regions of the open scaffold suffered greater stress, while the anterior and lateral areas of the articular surface and regions near the inlay rod and screw holes in the onlay plate also exhibited relatively high stress distributions.²⁸ These results implied that the reconstructive scaffold for bone defect should have regional variation consistent with trabecular microarchitecture, so that the reconstructed bone defect would have well biomechanical behaviors. Some studies showed that the precision of the selective laser sintering could reach 0.05 mm, which could be theoretically applied to mimic the microarchitecture properties of trabecular bone if the valuable morphological data of trabecular bone were referred to properly.²⁹⁻³¹ Therefore, analysis of the three-dimensional anatomical features could guide the design of the condyle prosthesis scaffold structure in the future by strengthening the number and thickness and increasing the trabecular bone porosity at specific regions of trabecular bone to optimize the design of the condylar prosthesis. The distribution features of the morphological parameters Tb.Th, Tb.N, BS/BV and Tb.Sp could also provide a reference for designing the scaffold of porous bone structures for better biomechanical adaptability.

Willems *et al* studied condyle trabecular bone in pigs and found that the morphology of trabecular bone changed with an increase in age.³² Although the bone volume fraction did not change significantly, Tb.Th increased, Tb.N decreased, and trabecular separation increased. In this study, donors were older, therefore, the influence of age on the structure of condyle trabecular bone was not analyzed.

This study proposed a method to analyze the three-dimensional detailed anatomical features of trabecular bone based on a VOI analysis. The morphological distribution of VOIs was anisotropic within trabecular bone of human condyles. The upper and lower ends of trabecular bone were much more compact, with higher BMD, Tb.Th, and Tb.N than the middle layers. The anterior part of trabecular bone was much more compact, with higher BMD, Tb.Th, and Tb.N than the posterior part. In the first, second and third layers, the medial part of trabecular bone was much more compact, with BMD, Tb.Th, and Tb.N than the lateral part. However, in the fourth, fifth and sixth layers, the lateral part of the trabecular bone was much more compact, with higher BMD, Tb.Th, and Tb.N than the medial part. As a result, regional analysis of mandibular condyle trabecular bone based on the VOIs offered additional information on radiological anatomy, facilitating analysis of the biomechanical properties of trabecular bone, and providing a reference for further design of the open porous scaffold to fabricate the trabecula architecture within the condyle.

Contributors

FL: Conceptualization, Methodology, Software, Validation, Formal analysis, Investigation, Data Curation, Writing - Original Draft. XX: Conceptualization, Methodology, Software, Validation, Formal analysis, Investigation, Data Curation, Writing - Original Draft. QR: Conceptualization, Methodology, Supervision. JW: Resources, Supervision. JZ: Software, Formal analysis, Investigation. WZ: Methodology, Software, Resources. WZ: Conceptualization, Resources, Writing - Review & Editing Visualization, Supervision. CG: Conceptualization, Writing - Review & Editing Visualization, Supervision, Funding acquisition.

Funding

This work was supported by the Beijing Municipal Science & Technology Commission (grant number Z201100005520055) and the Clinical Scientist Program, Peking University (grant number BMU2019LCKXJ009).

REFERENCES

1. Tanaka E, Koolstra JH. Biomechanics of the temporomandibular joint. *J Dent Res* 2008; **87**: 989–91. <https://doi.org/10.1177/154405910808701101>
2. Koolstra JH. Biomechanical analysis of the influence of friction in jaw joint disorders. *Osteoarthritis Cartilage* 2012; **20**: 43–48. <https://doi.org/10.1016/j.joca.2011.10.009>
3. van Ruijven LJ, Giesen EBW, Mulder L, Farella M, van Eijden TMGJ. The effect of bone loss on rod-like and plate-like trabeculae in the cancellous bone of the mandibular condyle. *Bone* 2005; **36**: 1078–85. <https://doi.org/10.1016/j.bone.2005.02.018>
4. Wolff J. *Das Gesetz der Transformtion der Knochen*. Berlin: Hirschwald; 1892.
5. Feldkamp LA, Goldstein SA, Parfitt AM, Jesion G, Kleerekoper M. The direct examination of three-dimensional bone architecture in vitro by computed tomography. *J Bone Miner Res* 1989; **4**: 3–11. <https://doi.org/10.1002/jbmr.5650040103>
6. Buxsein ML, Boyd SK, Christiansen BA, Guldberg RE, Jepsen KJ, Müller R. Guidelines for assessment of bone microstructure in rodents using micro-computed tomography. *J Bone Miner Res* 2010; **25**: 1468–86. <https://doi.org/10.1002/jbmr.141>
7. Ulm CW, Kneissel M, Hahn M, Solar P, Matejka M, Donath K. Characteristics of the cancellous bone of edentulous mandibles. *Clin Oral Implants Res* 1997; **8**: 125–30. <https://doi.org/10.1034/j.1600-0501.1997.080207.x>
8. Ebrahim FH, Ruellas ACO, Paniagua B, Benavides E, Jepsen K, Wolford L, et al. Accuracy of biomarkers obtained from cone beam computed tomography in assessing the internal trabecular structure of the mandibular condyle. *Oral Surg Oral Med Oral Pathol Oral Radiol* 2017; **124**: 588–99. <https://doi.org/10.1016/j.oooo.2017.08.013>
9. Nicolielo LFP, Van Dessel J, Jacobs R, Quirino Silveira Soares M, Collaert B. Relationship between trabecular bone architecture and early dental implant failure in the posterior region of the mandible. *Clin Oral Implants Res* 2020; **31**: 153–61. <https://doi.org/10.1111/clr.13551>
10. Du J, Brooke-Wavell K, Paggiosi MA, Hartley C, Walsh JS, Silberschmidt VV, et al. Characterising variability and regional correlations of microstructure and mechanical competence of human tibial trabecular bone: an in-vivo HR-pqct study. *Bone* 2019; **121**: 139–48. <https://doi.org/10.1016/j.bone.2019.01.013>
11. Renders GAP, Mulder L, van Ruijven LJ, van Eijden TMGJ. Porosity of human mandibular condylar bone. *J Anat* 2007; **210**: 239–48. <https://doi.org/10.1111/j.1469-7580.2007.00693.x>
12. Choi DY, Sun KH, Won SY, Lee JG, Hu KS, Kim KD, et al. Trabecular bone ratio of the mandibular condyle according to the presence of teeth: a micro-CT study. *Surg Radiol Anat* 2012; **34**: 519–26. <https://doi.org/10.1007/s00276-012-0943-x>
13. Kim D-G, Jeong Y-H, Kosel E, Agnew AM, McComb DW, Bodnyk K, et al. Regional variation of bone tissue properties at the human mandibular condyle. *Bone* 2015; **77**: 98–106. <https://doi.org/10.1016/j.bone.2015.04.024>
14. Kim JE, Shin JM, Oh SO, Yi WJ, Heo MS, Lee SS, et al. The three-dimensional microstructure of trabecular bone: analysis of site-specific variation in the human jaw bone. *Imaging Sci Dent* 2013; **43**: 227–33. <https://doi.org/10.5624/isd.2013.43.4.227>
15. Giesen EB, van Eijden TM. The three-dimensional cancellous bone architecture of the human mandibular condyle. *J Dent Res* 2000; **79**: 957–63. <https://doi.org/10.1177/00220345000790041101>
16. Hongo T, Yotsuya H, Shibuya K, Kawase M, Ide Y. *Quantitative and morphological studies on the trabecular bones in the condyloid processes of the Japanese mandibles. Comparisons between dentulous and edentulous specimens*. Bull Tokyo Dent Coll; 1989, pp.67–76.
17. Solberg WK, Hansson TL, Nordström B. The temporomandibular joint in young adults at autopsy: a morphologic classification and evaluation. *J Oral Rehabil* 1985; **12**: 303–21. <https://doi.org/10.1111/j.1365-2842.1985.tb01285.x>
18. Schlueter B, Kim KB, Oliver D, Sortiropoulos G. Cone beam computed tomography 3D reconstruction of the mandibular condyle. *Angle Orthod* 2008; **78**: 880–88. <https://doi.org/10.2319/072007-339.1>
19. Jiang H, Li C, Wang Z, Cao J, Shi X, Ma J, et al. Assessment of osseous morphology of temporomandibular joint in asymptomatic participants with chewing-side preference. *J Oral Rehabil* 2015; **42**: 105–12. <https://doi.org/10.1111/joor.12240>
20. Zhang LZ, Meng SS, He DM, Fu YZ, Liu T, Wang FY, et al. Three-dimensional measurement and cluster analysis for determining the size ranges of chinese temporomandibular joint replacement prosthesis. *Medicine (Baltimore)* 2016; **95**: e2897. <https://doi.org/10.1097/MD.0000000000002897>
21. Zhao Q, Sun N, Zhang F, Song D, Lu Z. Measurement of temporomandibular joint and surrounding accessory structures. *Journal of Shandong University Health Sciences* 2019; **57**: 87–91.
22. Guo XL, Liu R, Wang YX. Topology optimization of bionic porous structure based on biomechanical properties of trabecular bone. *Journal of Medical Biomechanics* 2018; **33**: 402–9.
23. Mitra E, Rubin C, Qin YX. Interrelationship of trabecular mechanical and microstructural properties in sheep trabecular bone. *J Biomech* 2005; **38**: 1229–37. <https://doi.org/10.1016/j.jbiomech.2004.06.007>
24. Goulet RW, Goldstein SA, Ciarelli MJ, Kuhn JL, Brown MB, Feldkamp LA. The relationship between the structural and orthogonal compressive properties of trabecular bone. *J Biomech* 1994; **27**: 375–89. [https://doi.org/10.1016/0021-9290\(94\)90014-0](https://doi.org/10.1016/0021-9290(94)90014-0)
25. Saers JPP, Cazorla-Bak Y, Shaw CN, Stock JT, Ryan TM. Trabecular bone structural variation throughout the human lower limb. *J Hum Evol* 2016; **97**: 97–108. <https://doi.org/10.1016/j.jhevol.2016.05.012>
26. Arahira T, Maruta M, Matsuya S, Todo M. Development and characterization of a novel porous β -TCP scaffold with a three-dimensional PLLA network structure for use in bone tissue engineering. *Materials Letters* 2015; **152**: 148–50. <https://doi.org/10.1016/j.matlet.2015.03.128>
27. Zhang K, Fan YB, Dunne N, Li XM. Effect of microporosity on scaffolds for bone tissue engineering. *Regen Biomater* 2018; **5**: 115–24. <https://doi.org/10.1093/rb/rby001>
28. Xu X, Luo D, Guo C, Rong Q. A custom-made temporomandibular joint prosthesis for fabrication by selective laser melting: finite element analysis. *Med Eng Phys* 2017; **46**: 1–11. <https://doi.org/10.1016/j.medengphy.2017.04.012>
29. Li SL. Comparative analysis of different 3D printing technology. *China Foundry Machinery & Technology* 2016; **6**: 6–8.
30. Pu YS, Wang BQ, Zhang LG. Metal 3D printing technology. *Surface Technology* 2018; **3**: 78–84.
31. Wang ZY, Chen YP. A survey on the metal additive manufacturing technology. *Die and Mould Technology* 2020; **1**: 59–63.
32. Willems NMBK, Mulder L, Langenbach GEJ, Grünheid T, Zentner A, van Eijden TMGJ. Age-related changes in microarchitecture and mineralization of cancellous bone in the porcine mandibular condyle. *J Struct Biol* 2007; **158**: 421–27. <https://doi.org/10.1016/j.jsb.2006.12.011>